J Mater Sci (2006) 41:5017–5020
DOI 10.1007/s10853-006-0135-3

LETTER

Self-assembled Nb_2O_5 microcones with tailored crystallinity

Robert L. Karlinsey

Received: 21 December 2005 / Accepted: 29 December 2005 / Published online: 27 May 2006

Metal oxides have found tremendous applications in numerous fields ranging from optical [1] and electronic [2] components in the form of electrochromic devices [3] and capacitors [4] to biocompatible, bioactive coatings on orthopedic implant materials [5, 6]. Titania [7–10] and alumina [11–14] are among the most widely studied metal oxides, and niobium oxide, for example, is considered a valuable candidate for biomaterial applications [15] due in part to its chemical inertness [16], thermodynamic stability [5] and low cytotoxicity [17]. While metal oxides can be formed through various methodologies, anodization of metal oxides offers a convenient, efficient and relatively inexpensive method in producing metal oxides. Driven by an external power source, this process expedites normal metal oxidation, thus increasing the rate of metal oxide formation. As a result, the fast kinetics generally produce a largely amorphous oxide material. Much research has therefore been reported on the amorphous nature of metal oxides [18, 19] and the properties thereof [11, 12, 19, 20], including niobium oxide [16, 21]. In this work, we report for the first time on the striking in situ evolution of crystalline niobium oxide microstructures, which is uncommon to the porous, tubular and needle-like morphologies reported on a variety of metal oxides [9, 13, 22–27]. Recently, an SEM investigation imaged the dependencies of these novel self-assembled microstructures on time, temperature, potential and HF(aq) electrolyte concentration [28]. The present study builds on the uniqueness of the microstructures by reporting on their modifiable crystalline character and morphology through addition of NaF to the HF(aq) electrolyte. The concept of coupling self-assembly with ordered phases offers an attractive avenue in the pursuit of tailored metal oxides for specific applications.

Evolution of niobium oxide in the present study is described as follows. 99.8% pure niobium foil 0.25 mm thick was purchased from Aldrich and HF acid (48% assay) was obtained from Fisher Scientific. The niobium metal was rinsed with acetone and ethanol and cut into one-centimeter wide strips. The acid was diluted with the appropriate amount of deionized water to achieve a concentration of 2.5 wt. % HF. The HF(aq) solutions contained either 0 or 100 mg of NaF salt (Aldrich). Anodization of the niobium metal was driven by a Sorensen DLM 300-2 power supply connected to copper and niobium metal electrodes. The electrodes were positioned in a 100 ml Nalgene beaker that contained the magnetically agitated electrolyte. A 20 V potential was employed to stimulate oxide development. Under these conditions changes in current were observed throughout anodization, indicating oxide rate forming processes.

Characterization of oxide morphology and composition oxide was performed using secondary electron imaging (SEI) and x-ray energy dispersive spectroscopy (EDS) using a JEOL JSM-5310LV scanning electron microscope. Figure 1 reveals representative cross-sectional images of the resulting niobium oxide structures anodized in HF(aq) electrolytes with (Fig. 1a) and without (Fig. 1b) NaF. Details of the microcone geometry have been described previously [28]. Both sets of structures in Fig. 1 were evolved at 40 °C, however, the structures in Fig. 1b required nearly twice as much time to grow relative to those in Figure 1a (i.e. ~1.75 h for the former, ~1 h for the latter). And while conical geometries are produced using

R. L. Karlinsey (✉)
Department of Preventive and Community Dentistry, Oral Health Research Institute, Indiana University School of Dentistry, 415 Lansing Street, Indianapolis, IN 46202, US
e-mail: rkarlins@iupui.edu

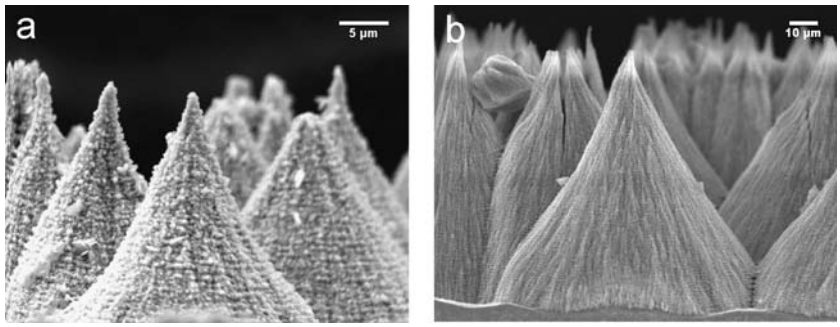

Fig. 1 Cross-sectional SEM images of niobium oxide cones anodized at 20 V in HF(aq) plus (**a**) 0 and (**b**) 100 mg NaF electrolyte solution

both electrolytes, the morphology of the microcones differs substantially. The self-assembled microstructures in Fig. 1a seem to be comprised of small crystallites, randomly oriented along each microbody: this assembly most likely contributes to the coarse texture and prevalence of microscopic groves and gaps. On the other hand, the microbodies in Fig. 1b display smoother texture, finer microtips, and large, well-aligned oxide 'fibers'. The composition of the niobium oxide has previously been verified for structures grown in HF(aq) and presently it is shown for HF(aq) + NaF in the EDS spectrum in Fig. 2. While the EDS analysis shows contributions from Nb, O and F, the spectrum does not provide evidence of Na in the oxide structure and it is nearly identical to that produced in HF(aq) (i.e. with no NaF) [28]. Thus, it seems that the presence of NaF strongly influences the kinetics and morphology of oxide growth without contributing a compositional change in the evolution of niobium oxide.

Since marked differences were observed in the spatial and temporal growth details of the niobium oxide microbodies in Fig. 1, X-ray diffraction (XRD) was used to explore the long-range order of the oxide. XRD patterns were collected

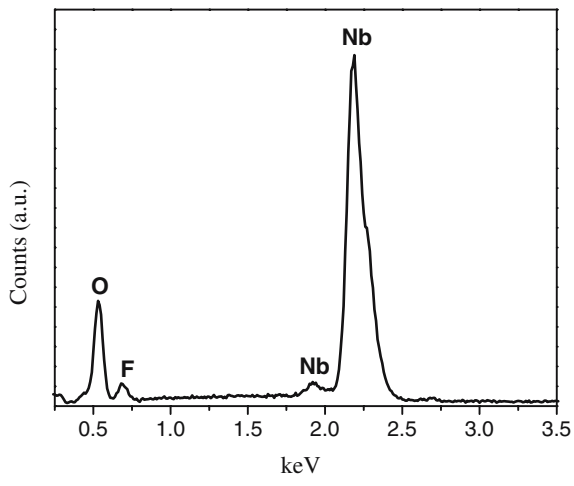

Fig. 2 EDS spectrum of niobium oxide anodized in HF(aq) + NaF electrolyte showing elemental contributions from O, F and Nb

on Siemens 5000 automated powder diffractometer with a 0.02° 2θ step-size operating at 40 kV/30 mA and are presented in Fig. 3. Figure 3a shows the XRD pattern for niobium oxide anodized in HF(aq).Using Bruker EVA software, the pattern was fingerprinted to orthorhombic Nb_2O_5 (JCPDS card # 27–1003). Remarkably, the XRD pattern reveals substantial crystallinity and contrasts markedly to previous work on niobium and other metal (e.g. titanium and aluminum) oxides formed via anodization processes [9, 13, 22–27]; typically, the resulting oxides are amorphous and require thermal treatments to induce crystallinity [2, 5, 6, 29]. The diffusion-limited rate of oxygen dissolution into the oxide (discussed below) [16, 21] coupled with oxide dissolution via HF may account for the development of small crystals.

When NaF is added to the HF(aq) electrolyte, microcone formation kinetics were observed to slow significantly. In addition to morphological changes, the XRD pattern in Fig. 3b further demonstrates the results of this effect. In Fig. 3b the intensity of the features near 22.6° and 36.8° 2θ are especially pronounced compared to those in Fig. 3a. Among the three sets of lineshapes, a most prominent change is observed for the lineshape near 22.6°, which contains the (001) plane, corresponding to the fiber axis of Nb_2O_5 ($c \sim 29.2$ Å). This augmented lineshape indicates development of large crystals along (001) and helps explain the morphological features shown in Fig. 1b and discussed above. The fact that Na was not observed in the oxide via EDS analysis suggests the following role of NaF. Since NaF is highly soluble, the salt readily dissociates enabling hydrolysis of F^- to form HF (weak acid) and OH^-, which slightly elevates the pH. Although this may alter the kinetics of dissolution and oxide formation, the substantial increase in crystal size may also be attributed to the solvation of Na^+ by up to six H_2O molecules. Under aqueous conditions, anodization stimulates the development of oxygen anions (i.e. from OH^-, O_2 or H_2O), which diffuse and react with mobile niobium ions according the hypothetical equations:

$$H_2O \rightarrow 2H^+ + O_2^- \quad (1)$$

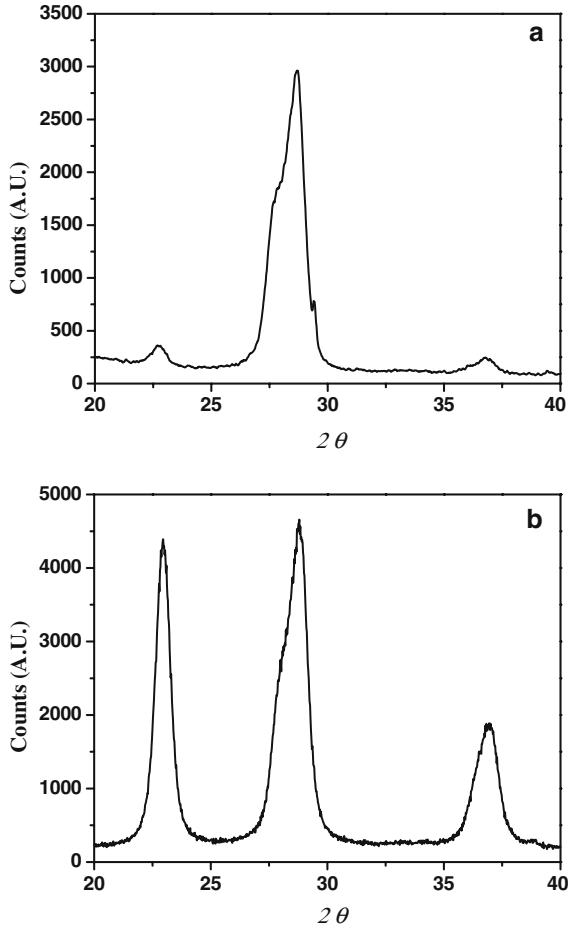

Fig. 3 XRD patterns of niobium oxide anodized in HF(aq) plus (**a**) 0 and (**b**) 100 mg NaF electrolyte solution

$$2Nb^{5+} + 5O^{2-} \rightarrow Nb_2O_5 \quad (2)$$

We speculate that water coordination to Na^+ modifies the thermodynamic potential for the reaction between oxygen and niobium ions. This scenario would then impart limiting behavior on the rate and extent of oxide diffusion during oxide growth, leading to slower microcone self-assembly. Additionally, such controlled growth favors the development of larger crystals, as shown in the character of the XRD lineshapes in Fig. 3. Research has suggested anion diffusion drives oxide growth after the initial barrier oxide is formed, as in the oxide systems ZrO_2 and HfO_2, where mobile oxygen anions dominate ionic transport [30]. This limit is consistent with the range in Nb^{5+} transport numbers during anodization (i.e. 0.22–0.33) [26]. It is important to note that we performed separate experiments with varied NaF and found longer anodization times were required at higher NaF content (e.g. 250 mg) in order to produce microcones of the same size. Therefore, the same type of effect discussed above is probably manifested in Nb_2O_5 evolution in this study. Incorporation of NaF (or similar salt) to the electrolyte thus imparts significant influence on the rate of oxide formation (i.e. degree of crystallization), even during a rapidly oxidizing experiment such as anodization.

In conclusion, we have discussed the morphology and phase of self-assembled Nb_2O_5 microbodies formed in an HF(aq) electrolyte using SEM and XRD. To the best of our knowledge this is the first time in situ crystallization of a self-assembled metal oxide phase via an anodization process has been reported. Additionally, we show larger crystals of the Nb_2O_5 orthorhombic phase can be obtained through addition of a salt (e.g. NaF) to the electrolyte. This study provides an economical and efficient method in producing crystalline Nb_2O_5 and may implicate other metals (e.g. Al, Ti), as well as bear on potential applications in medical, dental and materials science.

References

1. Sim H, Choi D, Lee D, Hasan M, Samantaray CB, Hwang H (2005) Microelect Eng 80:260
2. Ristic M, Popovic S, Music S (2004) Mat Lett 58:2658
3. Orel B, Krasovec UO, Macek M, Svegl F, Stangar UL (1999) Solar Energy Mater & Solar Cells 56:343
4. Choosuwan H, Guo R, Bhalla AS (2002) Mat Lett 54:269
5. Velten D, Eisenbarth E, Schanne N, Breme J (2004) J Mat Sci: Mat Med 15:457
6. Uchida M, Kim H-M, Kokubo T, Fujibayashi S, Nakamura T (2003) J Biomed Mat Res A 64:164
7. Cai Q, Paulose M, Varghese OK, Grimes CA (2005) J Mat Res 20:230
8. Macak JM, Sirotona K, Schmuki P (2005) Electrochimica Acta 50:3679
9. Gong D, Grimes CA, Varghese OK, Hu W, Singh RS, Chen Z, Dickey EC (2001) J Mat Res 16:3331
10. Mor GK, Shankar K, Paulose M, Varghese OK, Grimes CA (2005) Nano Lett 5:191
11. Keller F, Hunter MS, Robinson DL (1953) J Electrochem Soc 100:411
12. Brock AJ, Wood GC (1967) Electrochimica Acta 12:395
13. Li AP, Muller F, Birner A, Nielsch K, Gosele U (1998) J Appl Phys 84:6023
14. Popat KC, Mor G, Grimes CA, Desai TA (2004) Langmuir 20:8035
15. Miyazaki T, Kim H-M, Kokubo T, Ohtsuki C, Nakamura T (2001) J Ceramic Soc Jpn 109:929
16. Halbritter J (1987) Appl Phys A 43:1
17. Zwilling V, Darque-Ceretti E, Boutry-Forveille A, David D, Perrin MY, Aucouturier M (1999) Surf Interface Anal 27:629
18. O'Sullivan JP, Wood GC (1970) Proc R Soc London. Series A, Math Phys Sci 317:511
19. Young L (1961) Anodic oxide films, Academic Press, London
20. Fromhold AT Jr, Cook EL (1967) Phys Rev 158:600

21. Grundner M, Halbritter J (1984) Surface Science 136:144–154
22. Tsuchiya H, Macak JM, Sieber I, Taveira L, Ghicov A, Sirotona K, Schmuki P (2005) Electrochem Commun 7:295
23. Tsuchiya H, Schmuki P (2005) Electrochem Commun 7:49
24. Mor GK, Varghese OK, Paulose M, Mukherjee N, Grimes CA (2003) J Mat Res 18:2588
25. Lee WJ, Smyrl WH (2005) Electrochem Solid-State Lett 8:B7
26. Lu Q, Hashimoto T, Skeldon P, Thompson GE, Habazaki H, Shimizu K (2005) Electrochem Solid-State Lett 8:B17
27. Masuda H, Fukuda K (1995) Science 268:1466
28. Karlinsey RL (2005) Electrochem Commun 7:1190
29. Kim H-M, Miyaji F, Kokubo T, Nakamura T (1996) J Biom Mat Res 32:409
30. Leach JSL, Pearson BR (1988) Corr Sci 28:43